We are IntechOpen,
the world's leading publisher of
Open Access books
Built by scientists, for scientists

6,900
Open access books available

185,000
International authors and editors

200M
Downloads

154
Countries delivered to

Our authors are among the

TOP 1%
most cited scientists

12.2%
Contributors from top 500 universities

CLARIVATE ANALYTICS

BOOK CITATION INDEX

INDEXED

WEB OF SCIENCE™

Selection of our books indexed in the Book Citation Index
in Web of Science™ Core Collection (BKCI)

Interested in publishing with us?
Contact book.department@intechopen.com

Numbers displayed above are based on latest data collected.
For more information visit www.intechopen.com

Detect Structural Features of Asymmetric and Symmetric CH₂ and CH₃ Functional Groups and Their Ratio of Biopolymers Within Intact Tissue in Complex Plant System Using Synchrotron FTIRM and DRIFT Molecular Spectroscopy

Peiqiang Yu, PhD.
College of Agriculture and Bioresources, University of Saskatchewan
51 Campus Drive, Saskatoon, S7N 5A8
Canada

1. Introduction

1.1 Bright synchrotron radiation

Synchrotron light is photon beam, which is million times brighter than sunlight. A synchrotron facility is a giant particle accelerator that turns electrons into light (Wikipedia, 2010). How a Synchrotron Works? Electric Gun (EG: *Synchrotron Component 1*) in a synchrotron blasts out electrons. The electrons are accelerated to nearly speed of light by Linear Accelerator (LA: *Synchrotron Component 2*). A small synchrotron orbiting Booster Ring (BR: *Synchrotron Component 3*) increase their energy. Finally electron bunches enter Storage Ring (SR: *Synchrotron Component 4*). The bunches orbit ring controlled by serial magnets. Special magnet called "Undulator" causes electrons to rapidly change course and vast emitting energy in form of photons. Then photons enter Beamline (BL: *Synchrotron Component 5*) and directed to device called "monochromator" which selects specific wavelength required for each experiment. Finally, light focus onto sample at Experimental End Station (ES: *Synchrotron Component 6*), where scientists collect data to determine molecular structure (Dumas, 2003; Marinkovic et al., 2002; Miller, 2009; CLS, 2010; Wikipedia, 2010). The extremely bright synchrotron light makes it possible to detect biomaterial structure (make-up or conformation) at both molecular and cellular levels (Marinkovic & Chance, 2006; Miller & Dumas, 2006).

1.2 Probe molecular structure of biopolymer using synchrotron-based and DRIFT molecular spectroscopy

Snchrotron FTIR microspectroscopy has been developed as a rapid, direct, non-destructive and bioanalytical technique. This cutting-edge analytical technology is capable of exploring the molecular chemistry or structure of a biological tissue without destruction inherent structures at ultra-spatial resolutions (Dumas, 2003; Yu, 2004; Marinkovic & Chance, 2006; Miller & Dumas, 2006; Yu et al., 2008). This technique has been used for molecular imaging and mapping in plant/feed/food tissue (Yu et al., 2004; Marinkovic & Chance 2006; Miller &

Dumas 2006; Yu et al., 2007). The diffused reflectance infrared Fourier transform spectroscopy (DRIFT) molecular spectroscopy is capable of exploring the biopolymer conformation through molecular and functional group spectral analyses (Doiron et al., 2009a; Liu & Yu, 2010). It can be used to detect molecular structure changes in oil seeds affect by heat processing (Doiron et al., 2009b) and cereal grains after processing (eg bio-ethanol processing).

1.3 Objective of this article

In this article, a novel approach was introduced to study the molecular structural features of the asymmetric and symmetric CH_2 and CH_3 and their ratios of biopolymers in complex intact plant system. Recent progress and applications were reported on using synchrotron-based bioanalytical technique (SFTIRM) and DRIFT molecular spectroscopy to image ultraspatial distribution of intensities of the asymmetric and symmetric CH_2 and CH_3 functional groups in complex intact plant tissue and detect the effects of plant seed variety and bioethanol processing on plant-based biopolymer structure changes on a molecular basis in terms of the asymmetric and symmetric CH_2 and CH_3 functional groups.

2. Molecular structure and spectral features of biopolymer in complex pant system

2.1 Spectral characteristics of biopolymers in complex plant system

In complex plant system, the biopolymers which are highly related to nutrient availability, including protein, lipid, structure and non-structural carbohydrates (cellulosic compounds, starch). These biopolymers have very unique structures, therefore resulting in unique spectral bands for each biopolymer. Fig. 1. showed a typical ultra-spatially resolved synchrotron-based FTIRM spectrum in complex plant tissue (aleurone layer tissue of sorghum with pixel size: 10 μm × 10 μm) in the mid-IR region ca. 4000-800 cm^{-1}.

The function groups of biopolymers in complex plant system included N-H and O-H stretch, C-H groups stretch, amide I and II, C=O carbonyl, CHO and cellulosic compounds. The protein amide I frequency band centered at 1650 cm^{-1} and amide II centered at ca. 1550 cm^{-1}, both of which arise from specific stretching and bending vibrations within the protein backbone (Jackson et al., 1989; Harris & Chapman, 1992; Jackson & Mantsch, 1995, 1996). The cellulosic compound band is centered at ca. 1245 cm^{-1}. The non-structural carbohydrate of starch is at ca. 1025 cm^{-1} (Wetzel et al., 1998, 2003).

2.2 Asymmetric and symmetric CH_2 and CH_3 groups and their ratio in complex plant system

In Fig. 1, the functional groups include C-H stretching group bands. These groups include (1) Asymmetric CH_3 stretching band; (2) Asymmetric CH_2 stretching band; (3) Symmetric CH_3 stretching band; and (4) Symmetric CH_2 stretching band. Fig. 2 shows the CH_3 and CH_2 asymmetric and symmetric stretching band features in typical ultra-spatially resolved synchrotron-based FTIRM spectrum in complex plant tissue (aleurone tissue of sorghum, pixel size: 10 μm × 10 μm) in the C-H stretch region ca. 3015-2780 cm^{-1} showing C-H function groups of biopolymers: CH_3 asymmetric stretch at ca. 2958 cm^{-1}, CH_2 asymmetric stretch at ca. 2934 cm^{-1}, CH_3 symmetric stretch at ca. 2874 cm^{-1} and CH_2 symmetric stretch of acyl chains at ca. 2851 cm^{-1} (Wetzel & LeVine 1999; Jackson & Mantsch, 2000). The ratios of

the infrared absorbance intensity peak height or area are obtained by the height or area under one functional group band divided by the height or area under another functional group band (Yu et al., 2005).
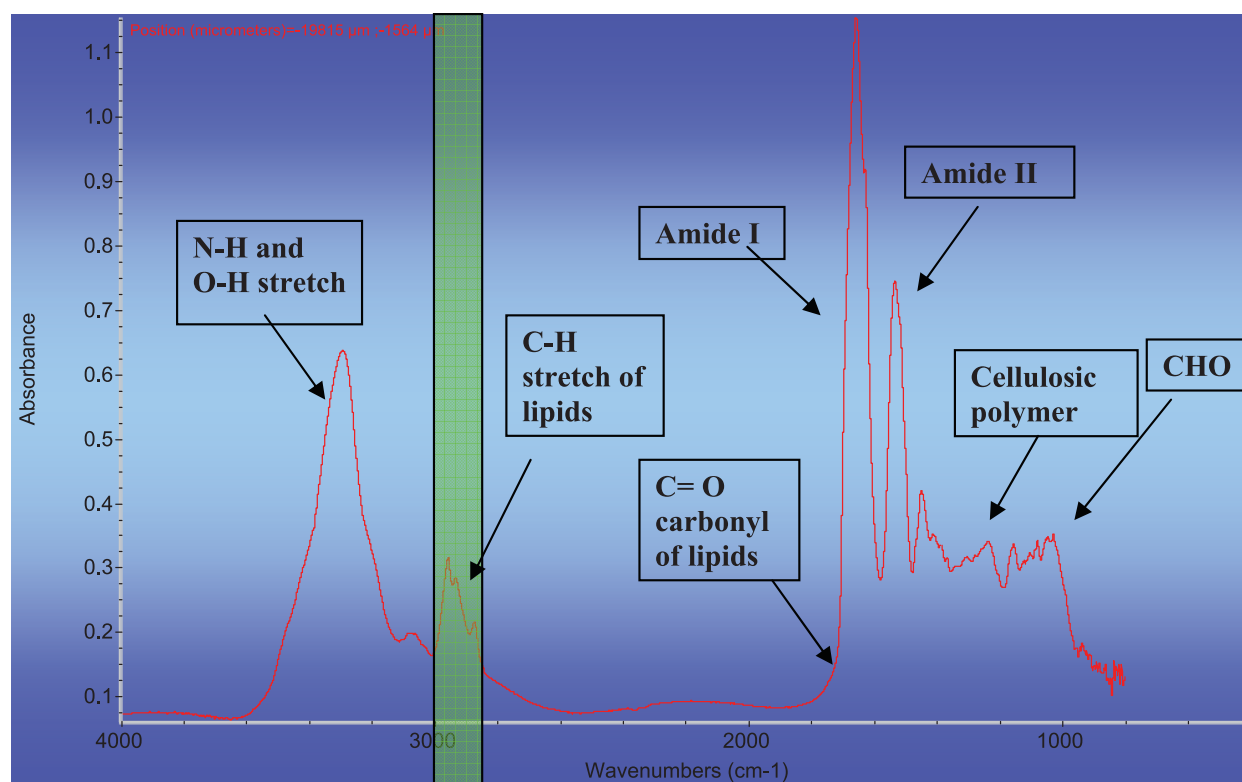

Fig. 1. Typical ultraspatially resolved synchrotron-based FTIRM spectrum in complex plant tissue (aleurone layer tissue of sorghum, pixel size: 10 μm × 10 μm) in the mid-IR region ca. 4000-800 cm^{-1} showed the function groups of biopolymers in complex plant system: N-H and O-H stretch, C-H groups stretch, amide I and II, C=O carbonyl, CHO and cellulosic compounds.

2.3 Molecular structure of a biopolymer in relation to nutrient availability

Nutrient availability of a biopolymer in animal and human is highly related to it molecular structure features (Walker et al., 2009). In an animal study (Doiron et al., 2009b), the protein molecular structure such as alpha-helix and beta-sheet ratio (Yu, 2006) highly associated with truly absorbed protein supply (metabolizable protein) in the small intestine to dairy cattle. Not only protein molecular structure but also amide I to II ratio in the new co-products of bioethanol processing also associated with true protein supply to dairy cattle.

3. Molecular imaging and molecular spectral analyses to discriminate and classify plant-based molecular structures in asymmetric and symmetric CH$_2$ and CH$_2$ groups

3.1 Imaging and mapping of asymmetric and symmetric CH groups in complex intact plant tissue

Using the synchrotron FTIR microspectroscopy, functional group images can be generated by plotting the intensity of synchrotron IR absorption bands as a function of xy position

(Budevska, 2002; Yu, 2005; Yu et al., 2007). Different coverage of the plant tissue with measurements could also be achieved by varying the step size and the dimensions of the image mask (aperture size). The big advantage of using synchrotron beam with FTIR spectroscopy to map the tissues is that diffraction limits and spatial resolution are achievable (Budevska, 2002; Wetzel et al., 1998). The false color maps were used (colors representing band intensities), which were derived from the area under particular spectral features.
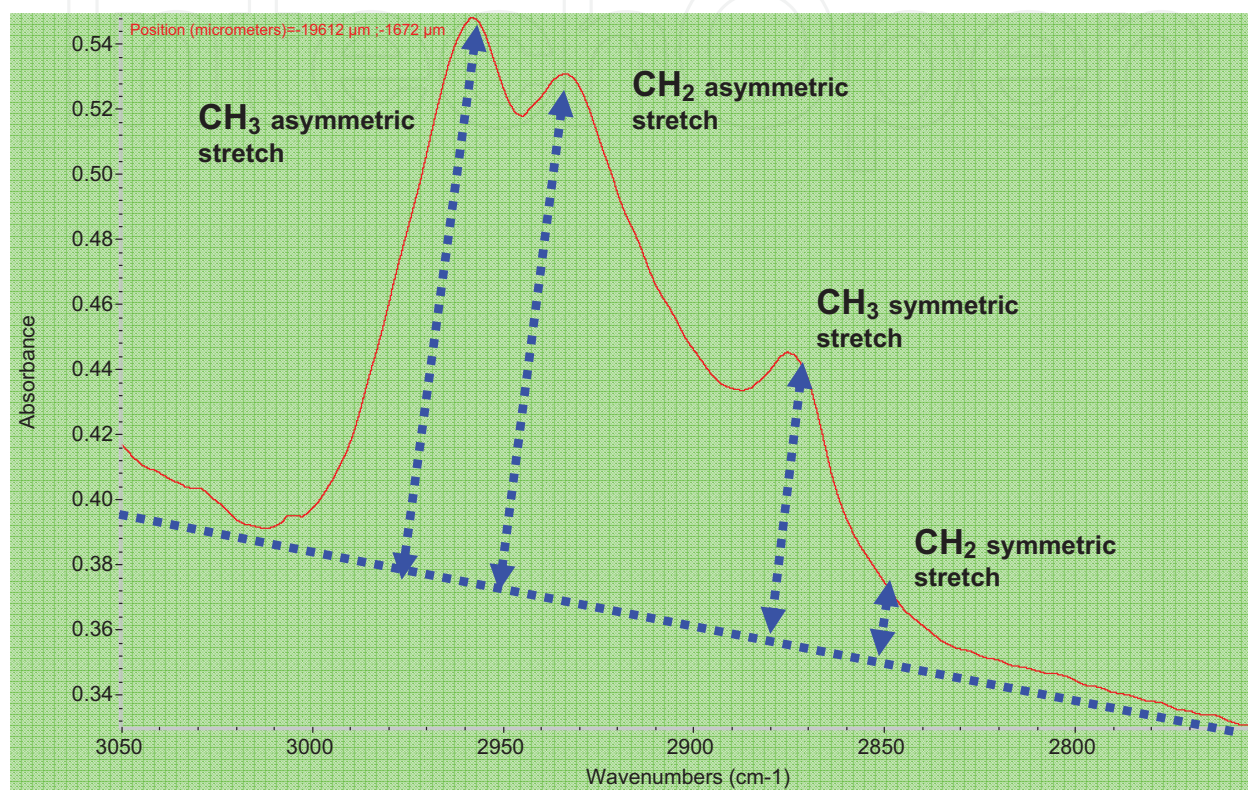
Fig. 2. The CH_2 and CH_3 asymmetric and symmetric stretching band features in typical ultra-spatially resolved synchrotron-based FTIRM spectrum in plant tissue (aleurone tissue of sorghum, pixel size: 10 μm × 10 μm) in the C-H stretch region ca. 3015-2780 cm^{-1} showing C-H function groups of biopolymers in complex plant tissue system: CH_3 asymmetric stretch at ca. 2958 cm^{-1}, CH_2 asymmetric stretch at ca. 2934 cm^{-1}, CH_3 symmetric stretch at ca. 2874 cm^{-1}, and CH_2 symmetric stretch at ca. 2851 cm^{-1}.

3.2 Agglomerative hierarchical molecular spectral cluster analysis

Agglomerative hierarchical cluster analysis (AHCA) is used to determine the main sources of variation in asymmetric and symmetric CH_2 and CH_3 groups spectra and the results are displayed as dendrograms using Ward's method (Cytospec Software). Doiron et al. (2009b) used AHCA analysis to detect the structure difference between the raw and heated treatment of flaxseed (cv. *Vimy*)

3.3 Spectral principle components analysis

Spectral Principle Components Analysis (PCA) used to determine major sources of variation in the asymmetric and symmetric CH_2 and CH_3 groups spectra. The purpose of PCA is to derive a small number of independent linear combinations (PCs) for a set of variables, while

retaining as much information in the original variables as possible. This analysis allows the global study of the relationships between a set of quantitative characters *p* (eg. chemical functional groups) observed for a set of *n* samples (eg. spectra). The outcome of such an analysis can be presented either as 2D (two PCs) or 3D (three PCs) scatter plots (Sockalingum et al., 1998).

4. Recent progress in asymmetric and symmetric CH$_3$ and CH$_2$ research in complex plant system

4.1 Application I: Imaging of spatial distribution of asymmetric and symmetric CH$_2$ and CH$_3$ groups with advanced synchrotron FTIR microspectroscopy

Using the synchrotron FTIR microspectroscopy, the functional group images of asymmetric and symmetric CH$_2$ and CH$_3$ in complex plant system can be generated within cellular and subcellular dimensions. Fig. 3 shows a visible image of the plant sorghum seed tissue. Fig. 4 shows plant CH functional group images (a) CH$_3$ asymmetric stretch at ca. 2960 cm^{-1}; (b) CH$_2$ asymmetric stretch at ca. 2929 cm^{-1}; (c) CH$_3$ symmetric stretch at ca. 2877 cm^{-1}; (d) CH$_2$ asymmetric stretch at ca. 2848 cm^{-1} of the plant sorghum seed tissue from the pericarp (outside), seed coat, aleurone layer and endosperm.
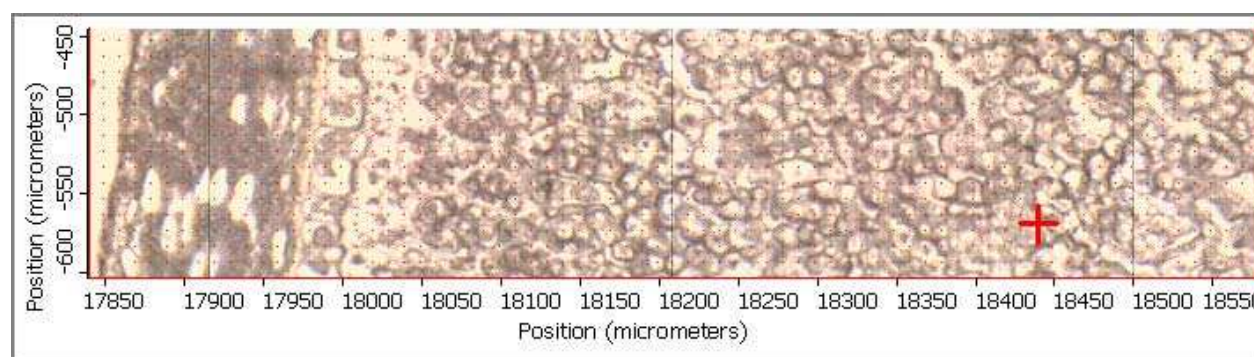

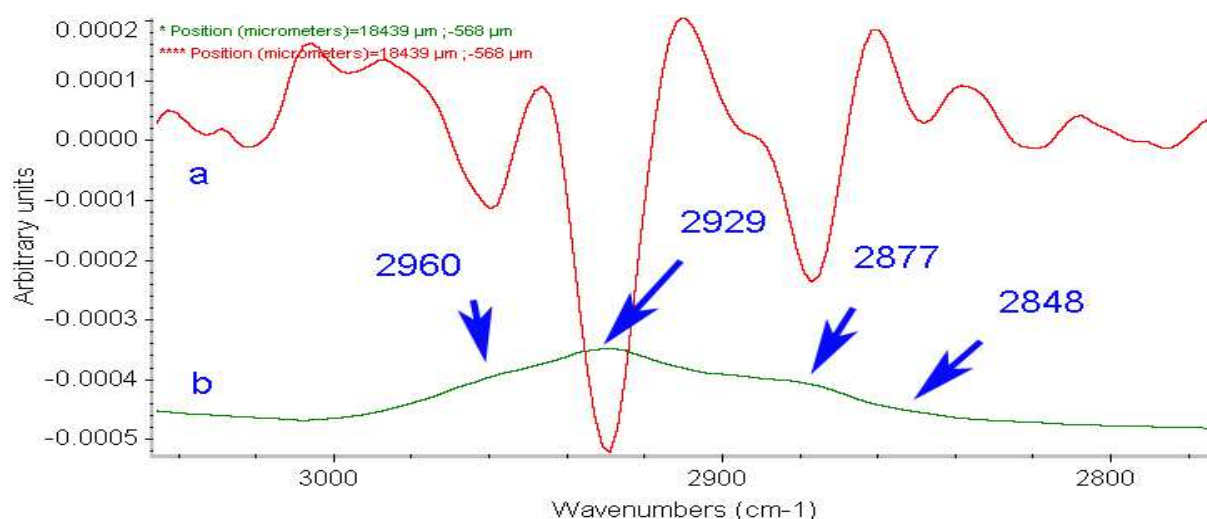Fig. 3a. A visible image of the plant sorghum seed tissue

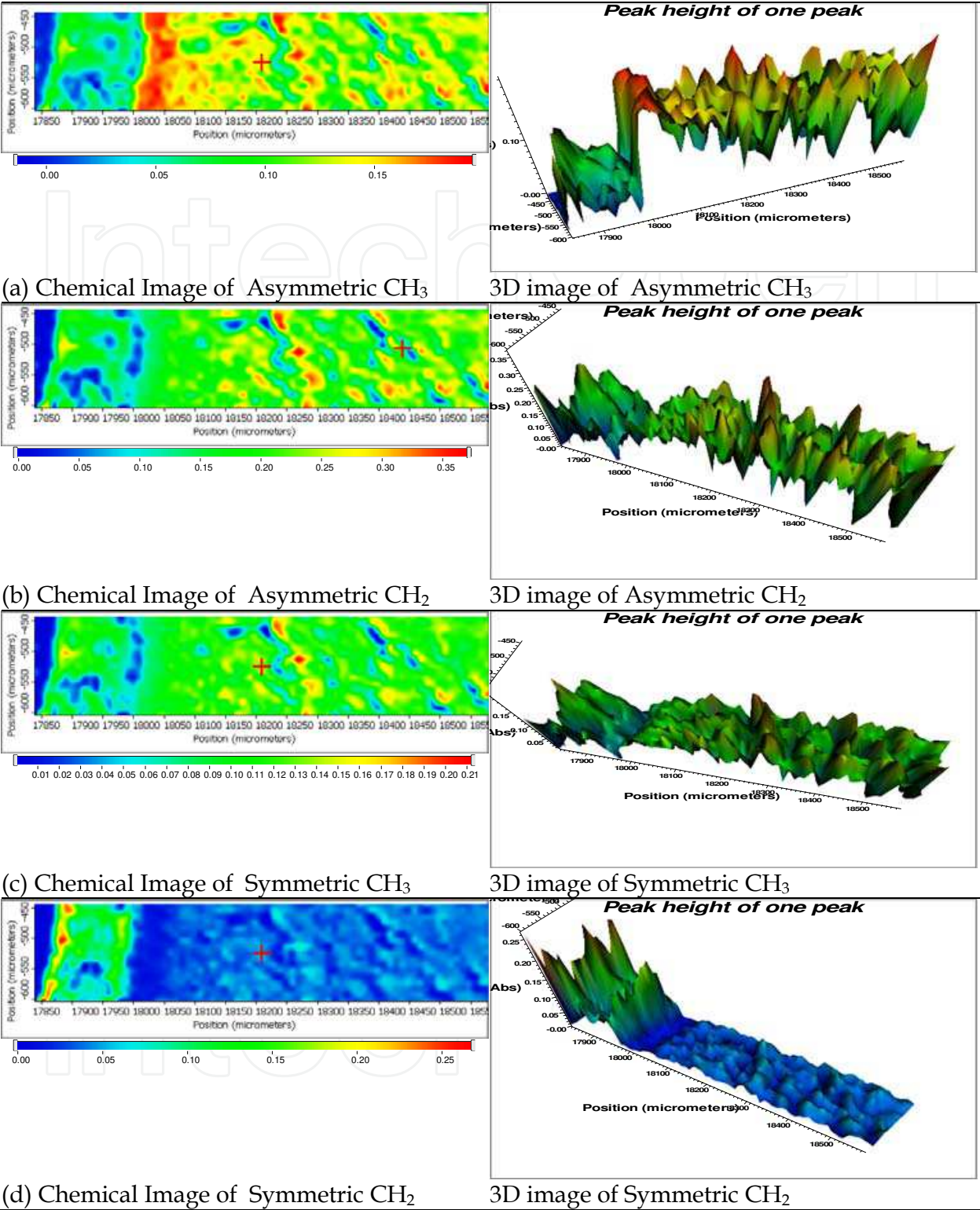Fig. 3b. Spectra corresponding to the pixel at the cross-hair in the visible image (spectrum pixel size 10 ×10 μm).

(a) Chemical Image of Asymmetric CH$_3$ 3D image of Asymmetric CH$_3$

(b) Chemical Image of Asymmetric CH$_2$ 3D image of Asymmetric CH$_2$

(c) Chemical Image of Symmetric CH$_3$ 3D image of Symmetric CH$_3$

(d) Chemical Image of Symmetric CH$_2$ 3D image of Symmetric CH$_2$

Fig. 4. CH functional group images [(a) CH$_3$ asymmetric stretch at ca. 2960 cm^{-1}; (b) CH$_2$ asymmetric stretch at ca. 2929 cm^{-1}; (c) CH$_3$ symmetric stretch at ca. 2877 cm^{-1}; (d) CH$_2$ asymmetric stretch at ca. 2848 cm^{-1}] of the sorghum seed tissue from the pericarp (outside), seed coat, aleurone layer and endosperm, using synchrotron-based FTIR microspectroscopy (1. Visible image; 2 Chemical image; 3. Spectra corresponding to the pixel at the cross-hair in the visible image) (spectrum pixel size 10 ×10 μm).

4.2 Application II: comparison of yellow- (*Brassica Rapa*) and brown-seeded (*Brassica Napus*) canola within cellular dimensions in structural features of asymmetric and symmetric CH$_2$ and CH$_3$, explored with advanced synchrotron FTIR microspectroscopy

This study aimed to use advanced synchrotron technique- SRFTIRM to compare two types of canola seed (yellow- (*Brassica Rapa*) vs. Brown-Seeded (*Brassica Napus*) Canola) at a cellular level in structural features of asymmetric and symmetric CH$_2$ and CH$_3$. The results showed the average absorbed peak intensities of CH functional groups: CH$_3$-asymmetric; CH$_2$-asymmetric; CH$_3$-symmetric; and CH$_2$-symmetric stretching vibrations of the yellow- and brown-seeded canola tissues, but no differences were found between the yellow- (*Brassica* rapa) and brown-seeded (*Brassica* napus) canola tissue, indicating similar CH$_2$ and CH$_3$ content between the two seed types. The peak height ratios of total CH$_2$:CH$_3$; CH$_3$-asymmetric: CH$_3$-symmetric; CH$_2$-asymmetric: CH$_2$-symmetric and total CH-asymmetric: CH-symmetric were 1.06 and 1.13, 1.28 and 1.26, 2.90 and 3.08, 1.82 and 1.78, for the yellow- and brown-seeded canola, respectively. Based on average data from each canola tissue, no significant differences were found, indicating that lipid chain length and branching is similar between the two seed types (Yu et al., 2005).

4.3 Application III: effect of bio-ethanol processing on structure changes of asymmetric and symmetric CH$_2$ and CH$_3$ on a molecular basis

Recently there is a dramatic increase in the bioethanol production which results in different types of co-products (Nuez-Ortín & Yu, 2009, 2010). This study aimed to reveal molecular structures of the new co-products of bioethanol production affected by bio-ethanol processing, identify the differences in asymmetric and symmetric CH$_2$ and CH$_3$ on a molecular basis between grains and new co-products and between different types of the bioethanol co-products. Fig. 4 (D. Damiran, personal communication) showed that the structural asymmetric and symmetric CH$_2$ and CH$_3$ groups were different between the grains and the new co-products of bio-ethanol production.

Cluster analyses (Fig. 5) indicated that the spectra of asymmetric and symmetric CH$_2$ and CH$_3$ between the grain (corn) and co-products of bioethnaol production (corn DDGS) were fully discriminated. This indicates that bioethanol processing change molecular structure of asymmetric and symmetric CH$_2$ and CH$_3$ conformation of the grain.

Fig. 6 show results from principal component analysis of the spectrum of asymmetric and symmetric CH$_2$ and CH$_3$. The first two PCs (obtained after data reduction) were plotted and show that the original grain (corn) and co-products of corn DDGS from bioethanol production can be grouped in separate ellipses. The first two PCs explain 99.98%, and 0.01 of the variation in the structural molecular spectrum data set between the corn and corn DDGS. Therefore principal component analysis show the distinguished difference between the corn and corn DDGS. These results indicate that the structural make-up in terms of asymmetric and symmetric CH$_2$ and CH$_3$ conformation between the corn and corn DDGS is fully distinguished.

5. Conclusions and implications

Using synchrotron-based SFTIRM and DRIFT molecular spectral spectroscopy, the structural feature and conformation of functional groups of asymmetric and symmetric CH$_2$
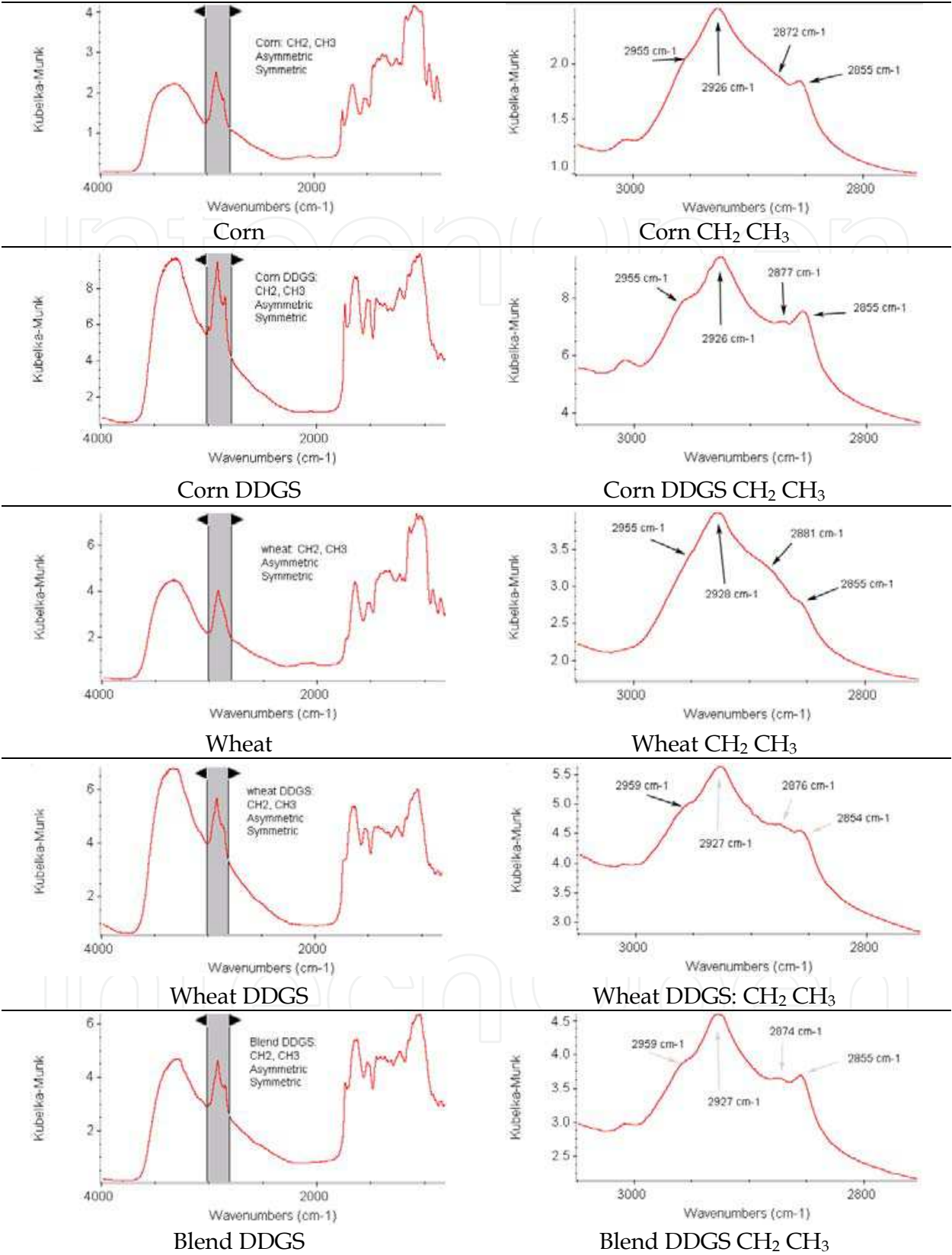
Fig. 4. Comparison of different types of DDGS and original feedstock in CH_3 and CH_2 asymmetric and symmetric stretching bands profiles using the DRIFT molecular spectroscopy: Effect of Bio-Ethanol Processing

Tree Diagram for 16 Cases: 1 - Corn DDGS, 6 - Corn
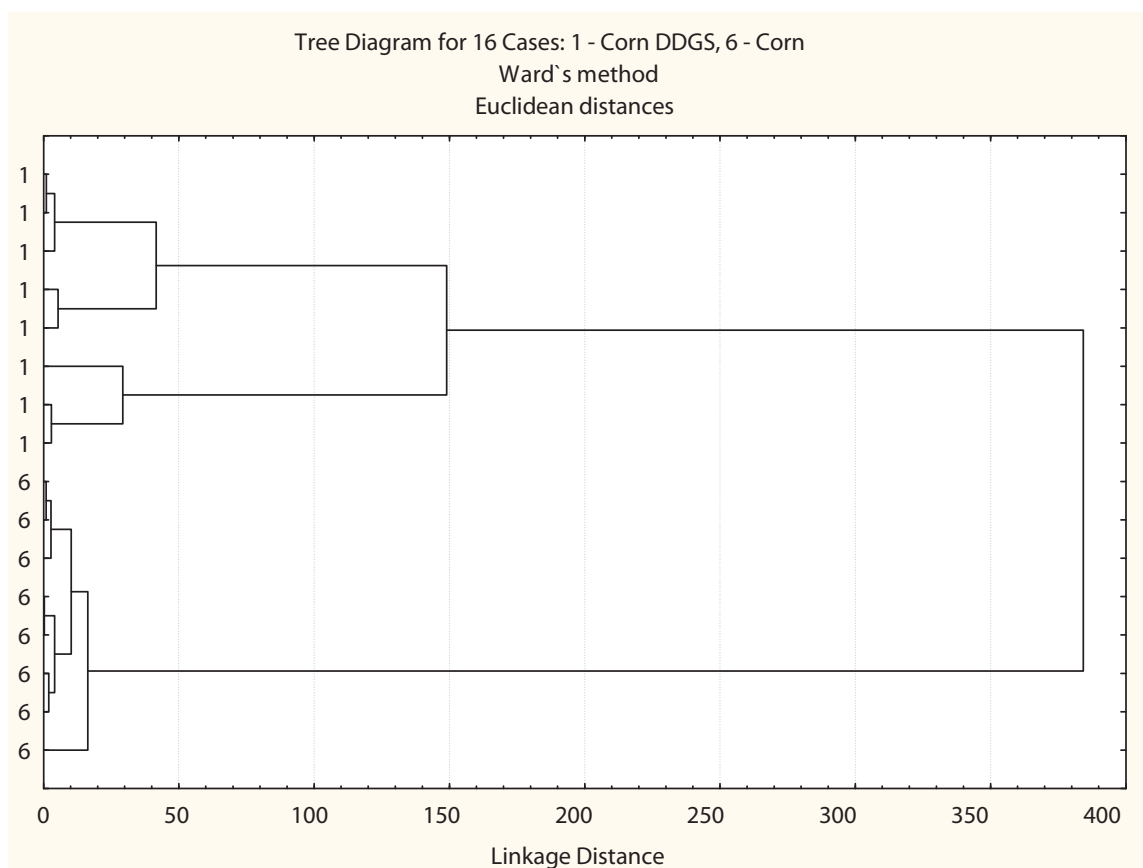Ward`s method
Euclidean distances

Fig. 5. Cluster analysis of spectrum detected with DRIFTS (acquired at 4 cm^{-1} resolution in the reflectance mode with subtraction of the KBr background, accumulated 256 times; range of wavenumbers, 3027-2813 cm^{-1}, IR reflectance Kubelka-Munk units) obtained from corn DDGS (1) vs. corn grain (6) from all original spot spectrum [CLA: (a) region of CH groups (CH_2, CH_3) ca. 3027-2813 cm^{-1}; (b) distance method, Euclidean; (c) cluster method, Ward's algorithm] (source: D. Damiran)

and CH_3 and their ratios (asymmetric CH_2 to symmetric CH_2 ratio; asymmetric CH_3 to symmetric CH_3 ratio; asymmetric CH_2 to asymmetric CH_3 ratio; symmetric CH_2 to symmetric CH_3 ratio) on a molecular basis could be detected in complex plant system. The molecular structure changes induced by various processing (eg. heating and bio-ethanol processing) or molecular structure difference between plant varieties could be revealed. The ultra-spatial distribution of the intensities of the asymmetric and symmetric CH_2 and CH_3 and their ratios could be imaged. The molecular structure difference between plant varieties or structure change induced by processing in terms of asymmetric and symmetric CH_2 and CH_3 and their ratios will affect functionality and nutrient availability and biodegradation in human and animals.
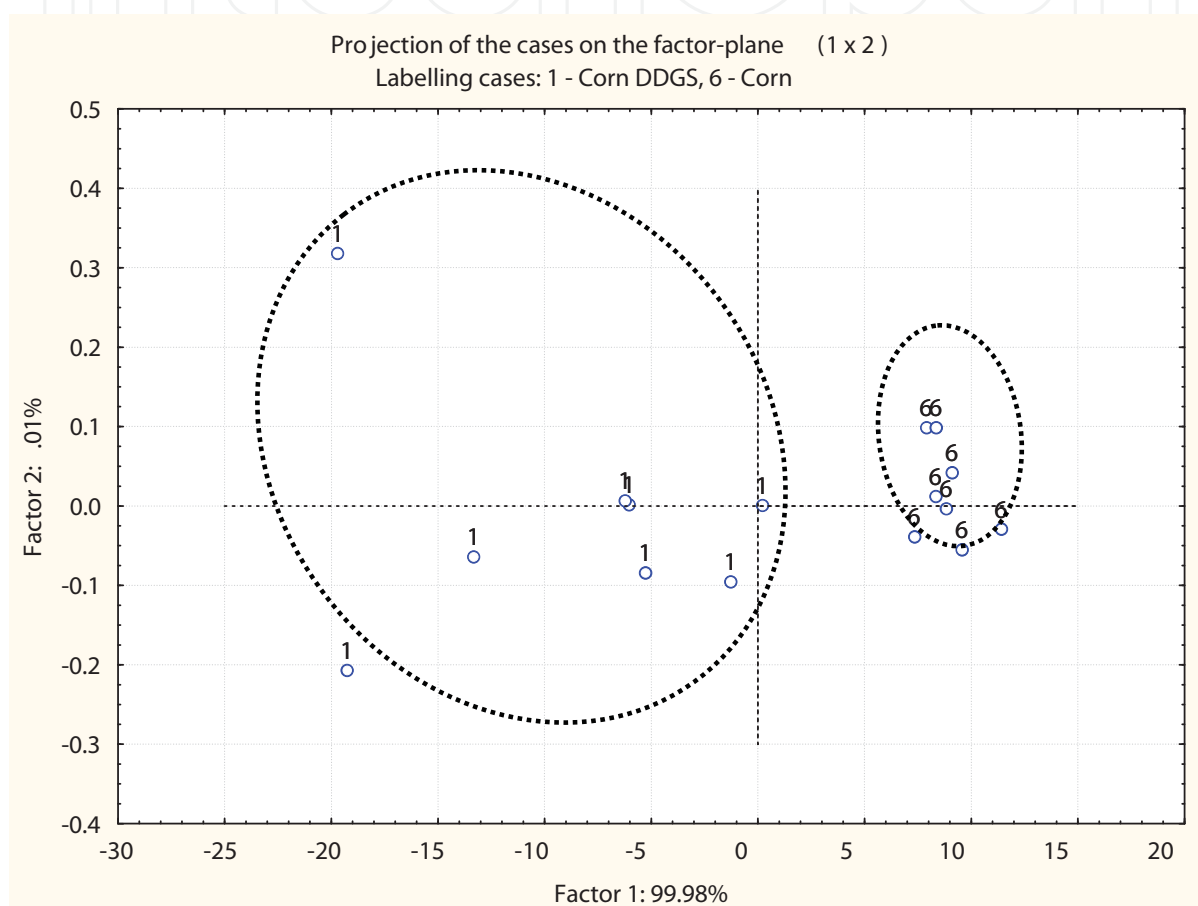
6. Acknowledgments

Fig. 6. Scatter plot of the 1st principal component vs. the 2nd principal component (a) of PCA analysis of spectrum detected with DRIFTS (acquired at 4 cm^{-1} resolution in the reflectance mode with subtraction of the KBr background, accumulated 256 times; range of wavenumbers, 3027–2813 cm^{-1}, IR reflectance Kubelka-Munk units) obtained from corn DDGS (1) vs. corn grain (6) from all original spot spectrum (CH groups (CH$_2$, CH$_3$) 3027-2813 cm^{-1}): The 1st and 2nd principal component explains 99.98, and 0.01% of the total variance, respectively (source: D. Damiran)

7. References

Budevska, B. O. (2002). Applications of Vibrational Spectroscopy in Life, Pharmaceutical and Natural Sciences. In: *Handbook of Vibrational Spectroscopy*, Vol. 5, Chalmers, J. M.

and P.R. Griffiths, P.R. (Ed.), pp 3720-3732. John Wiley and Sons, Inc., New York, NY, USA

CLS. (2010). Synchrotron facts. Available: http://www.lightsource.ca/education/whatis.php Accessed Mar, 2010.

Cytospec. Software for Infrared Spectral Imaging. V. 1.1.01

Damiran, D. & Yu, P. (2010). Structural make-up, biopolymer conformation and biodegradation characteristics of newly developed super genotype of oats (CDC SO-I vs. conventional varieties): A novel approach. *J Agric Food Chem*. 58: 2377-2387

Doiron, K. J. & Yu, P., Christensen, C. R., Christensen, D. A. & McKinnon, J. J. (2009a). Detecting molecular changes in *Vimy* flaxseed protein structure using synchrotron FTIRM and DRIFT spectroscopic techniques: structural and biochemical characterization. *Spectroscopy* 23: 307–322

Doiron, K. J., Yu, P., McKinnon, J. J., & Christensen, D. A. (2009b). Heat-induced protein structures and protein subfractions in relation to protein degradation kinetics and intestinal availability in dairy cattle. *J Dairy Sci* 92:3319-3330

Dumas, P. (2003). Synchrotron IR Microspectroscopy: A Multidisciplinary Analytical Technique. The 6th Annual Synchrotron CLS Users' Meeting and Associated Synchrotron Workshops University of Saskatchewan, Canada. Nov 13-15.

Harris, P. I. & Chapman, D. (1992). Does Fourier-transform infrared spectroscopy provide useful information on protein structures? *Trend Biochem Sci* 17: 328-333.

Jackson, M., Haris, P. I. & Chapman, D. (1989) Conformational transitions in poly-L-lysine: an FT-IR spectroscopic study. *Biochim Biophys Acta* 998:75.

Jackson, M. & Mantsch, H. H. (1995). The use and misuse of FTIR spectroscopy in the determination of protein structure. *Biochemistry and Molecular Biology* 30: 95-120.

Jackson, M. & Mantsch, H. H. (1996). Biomedical Infrared Spectroscopy, Pages 311-340 in Infrared Spectroscopy of Biomolecules, eds. HH. Mantsch, D. Chapman, Wiley-Liss, New York.

Liu, N. & Yu, P. (2010). Using DRIFT molecular spectroscopy with uni- and multivariate molecular spectral techniques to detect plant protein molecular structure difference among different genotypes of barley. *J Agric Food Chem*. In Review

Marinkovic, N. S. & Chance, M. R. (2006) Synchrotron Infrared Microspectroscopy. In: (Meyers R, ed) *Encyclopedia of Molecular Cell Biology and Molecular Medicine,* 2nd ed., Vol 13, Wiley Inc. pp 671-708.

Marinkovic, N. S., Huang, R., Bromberg, P., Sullivan, M., Toomey, J., Miller, L. M., Sperber, E., Moshe, S., Jones, K. W., Chouparova, E., Lappi, S., Franzen, S. & Chance, M. R. (2002). Center for Synchrotron Biosciences' U2B beamline: an international resource for biological infrared spectroscopy. *J Synchrotron Rad* 9:189-197.

Miller, L. M. (2009). Infrared Microsperctroscopy and Imaging. Available: http://nslsweb.nsls.bnl.gov/nsls/pubs/nslspubs/imaging0502/irxrayworkshopintroduction.ht Accessed Oct.

Miller, L. M. & Dumas, P. (2006). Chemical imaging of biological tissue with synchrotron infrared light. *Biochim Biophys Acta* 1758: 846-857.

Nuez-Ortín, W. G. & Yu, P. (2009). Nutrient variation and availability of wheat DDGS, corn DDGS and blend DDGS from bioethanol plants. *J Sci Food Agric*. 89: 1754–1761

Nuez-Ortín, W. G. & Yu, P. (2010). Effects of Bioethanol Plant and Co-products Type on the Metabolic Characteristics of the Proteins. *J Dairy Sci*. In press.

Sockalingum, G. D., Bouhedja, W., Pina, P., Allouch, P., Bloy, C. & Manfait, M. (1998). FT-IT spectroscopy as an emerging method for rapid characterization of microorganisms. *Cell Mol Bio* 44: 261-269.

Walker, A. M., Yu, P., Christensen, C. R., Christensen, D. A. & McKinnon, J. J. (2009). Fourier Transform infrared microspectroscopic analysis of the effects of cereal type and variety within a type of grain on molecular structural make-up in relation to rumen degradation kinetics. *J Agric Food Chem* 57: 6871–6878

Wetzel, D. L. & LeVine, S. M. (1999). Imaging molecular chemistry with infrared microscopy. *Science.* 285: 1224-1225.

Wetzel, D. L., Srivarin, P. & Finney, J. R. (2003). Revealing protein infrared specrtral detail in a heterogeneous matrix dominated by starch. *Vibrational Spectroscopy* 31: 109-114.

Wikipedia. (2010). Synchrotron light source. http://en.wikipedia.org/wiki/ Synchrotron_light_source. Accessed April.

Yu, P. (2004). Application of advanced synchrotron-based Fourier transform infrared microspectroscopy (SR-FTIR) to animal nutrition and feed science: a novel approach. British J Nutri 92: 869-885.

Yu, P., McKinnon, J. J., Christensen, C. R. & Christensen, D. A. (2004). Imaging Molecular Chemistry of Pioneer Corn. *J Agric Food Chem* 52:7345-7352

Yu, P., Christensen, C. R., Christensen, D. A. & McKinnon, J. J. (2005). Ultrastructural-chemical makeup of yellow- (*Brassica Rapa*) and brown-seeded (*Brassica Napus*) canola within cellular dimensions, explored with synchrotron reflection FTIR microspectroscopy. *Can J Plant Sci* 85: 533-541.

Yu, P., Block, H., Niu, Z. & Doiron, K. J. (2007). Rapid characterization of molecular chemistry and nutrient make-up and microlocalization of internal seed Tissue. *J Synchrotron Rad* 14: 382-390.

Yu, P., Doiron, K. & Liu, D. (2008) Shining light on the difference in molecular structural chemical make-up and the cause of distinct biodegradation behavior between malting- and feed-type barley: A novel approach. *J Agric Food Chem (Molecular Nutrition Section)* 56: 3417-3426.
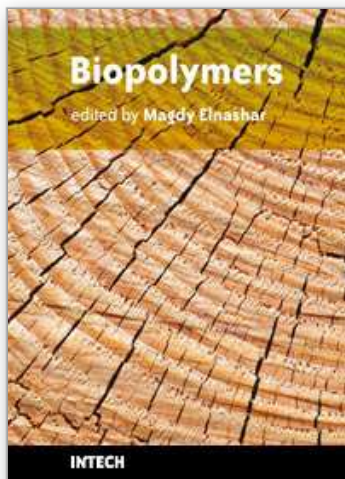
Biopolymers

Edited by Magdy Elnashar

ISBN 978-953-307-109-1

Hard cover, 612 pages

Publisher Sciyo

Published online 28, September, 2010

Published in print edition September, 2010

Biopolymers are polymers produced by living organisms. Cellulose, starch, chitin, proteins, peptides, DNA and RNA are all examples of biopolymers. This book comprehensively reviews and compiles information on biopolymers in 30 chapters. The book covers occurrence, synthesis, isolation and production, properties and applications, modification, and the relevant analysis methods to reveal the structures and properties of some biopolymers. This book will hopefully be of help to many scientists, physicians, pharmacists, engineers and other experts in a variety of disciplines, both academic and industrial. It may not only support research and development, but be suitable for teaching as well.

INTECH
open science | open minds